ELSEVIER

Contents lists available at ScienceDirect

Composites Part A

journal homepage: www.elsevier.com/locate/compositesa



Check for updates

Electrical curing of carbon fibre composites with conductive epoxy resins

Yunlong Tang*, J. Patrick A. Fairclough

The Department of Mechanical Engineering, The University of Sheffield, Sheffield S10 2TN, United Kingdom

ABSTRACT

Direct electric cure (DEC) was used to cure carbon fibre-reinforced polymers (CFRPs). We show that the energy consumption for curing is significantly reduced, with the judicious placement of contact electrodes, by almost twelve-fold, compared to autoclave curing, and threefold compared to oven curing (0.84, 10.0, and 2.64 kW). CFRP samples of an epoxy matrix with 0-3 wt% carbon black (CB) was used to increase matrix conductivity, and the effect of this variation on the curing and mechanical properties was determined. Subsequently, the concentration with the highest flexural strength, a CFRP with 2 wt% CB was prepared, to study the effects of four different contact arrangements (Top-Bottom, Outside-Outside, Outside-Inside, Inside-Inside) under high pressure (about 2 MPa). Top-Bottom mode shows the best performance, here the electrical current flows through the ply stack perpendicular to the fibre direction. This CFRP has similar mechanical properties as samples manufactured by a range of traditional curing methods. Although the degree of cure (DOC) was reduced by 3–7 %, dependent on the placement of the electrical contacts, the through ply cures showed uniform and high degrees of cure. We show that DEC, thus provides a low capital investment solution to high-quality composite manufacture, facilitating market access for small enterprises, as part sizes and curing times are not limited by oven size nor oven thermal mass.

1. Introduction

Carbon fibre-reinforced polymers (CFRP) have been widely used in many different fields, such as aerospace, transportation, and electronics [1,2,3,4,5]. These applications exploit CFRP's outstanding mechanical properties of high tensile strength and high stiffness but low density. Thermoset CFRPs are commonly epoxy resin-based as these are low-cost, high stiffness and chemically inert matrix materials. Traditional manufacturing methods use autoclaves, ovens, or heated presses to cure these epoxy resins. CFRP manufactured by these devices shows excellent properties, such as high-volume fractions of fibre and low porosities [5,6,7]. However, the dimensions of CFRP parts manufactured by these methods are limited by the chamber size [8]. The processing time is limited by the slow heating rates for parts manufactured by ovens and autoclave as these have high thermal masses. As a result, composite manufacture has traditionally required considerable expenditure both in terms of capital, to purchase the equipment, and in running costs to heat the ovens, moulds and parts.

The reason for these drawbacks is that the curing of CFRP requires heating the part within its mould to high temperatures to initiate and maintain curing. This requires a large input of energy, the majority of which is not used to cure the part but to heat the mould, the air within the chamber and/or the chamber itself [9]. This additional, parasitic, "thermal mass" creates a secondary issue for parts with thick sections. The exothermic curing polymerisation reaction releases heat. This causes the resin's temperature to rise, which in turn increases the rate of

heat release. This positive feedback process can lead to over-curing, degradation of the resin and even combustion in extreme cases. This is generally, but somewhat misleadingly, termed "exotherming" [10]. The large thermal mass of the oven or autoclave prohibits the rapid removal of heat required to control this process and thus the manufacturing guidelines often specify conservative, slow heating ramps to prevent "exotherms" in thick parts.

To improve production times and minimise cost it is therefore essential to reduce, as far as possible, the thermal mass of the system. This can be achieved by direct heating of the CFRP part. This has been achieved by the use of induction curing [11,12], microwave curing [13,14,15,16] and infrared radiation (IR) [17,18], which are all examples of electromagnetic curing methods. In induction heating, the frequency is low, 100 to 200 kHz [19]. Here magnetic induction induces eddy currents in the fibres, these powerful currents rapidly heat the composite. However, the orientation of the fibre to the induction coil is critical to ensure efficient energy transfer [2]. In multiple-ply stacks, this can mean that some plies may be heated to higher temperatures than adjacent plies. However, thermal diffusion will generally resolve this issue. These low frequencies can penetrate deeper into the material. As a result, induction heating curing is generally applied to manufacture thicker and more complex geometries. In addition, due to the limitation of the power transfer, the coil must be close to the area to be heated. This limits operational freedom and requires complex bespoke coils for curved parts with large dimensions [20]. Microwave uses frequencies between 300 MHz to 300 GHz, here the electromagnetic radiation

E-mail address: ytang52@sheffield.ac.uk (Y. Tang).

 $^{^{\}ast}$ Corresponding author.

interacts with dipoles in the resin. The oscillation of these dipoles induces heating within the material. Microwave curing is often subject to uneven temperature distribution with certain part shapes focussing or dispersing the microwaves. Additionally, sharp edges induce burning due to arcing as the field lines are concentrated at sharp points. [15,21]. Dipoles are again important in IR curing, at frequencies between 300 GHz – 430 THz. These high frequencies have poor penetration and thus thermal diffusion from the exposed surfaces to the core tends to limit IR curing to thin laminates and surface finishes. Additionally, infrared radiation curing particularly of irregular shapes may lead to non-uniform heating [8].

Carbon fibre is inherently conductive and therefore can act as its own heating element. Thus, direct electric cure (DEC) can be leveraged to produce a low-energy, highly controllable curing process that directly heats the composite part. Lee [22] indicates DEC can achieve a 99 % energy saving compared with autoclave curing. Fukuda *et al.* [23] introduced DEC (or Joule Heating) to fabricate thermoset CFRP parts. Utilizing two different contact arrangements and vacuum consolidation, they were able to examine through thickness heating and edge-to-edge heating.

However, DEC is not without issues. Large or complex geometries are difficult to implement in DEC due to the necessity to have electrical connections across the part [22,24,25,26]. Similarly, the need to balance the current density and thereby heating across the part can lead to variations in the cure across the part [27]. Collinson $et\ al.$ [8] used DEC to cure prepreg with vacuum consolidation for large areas, a sample size of 700×2000 mm with 16 plies thick prepreg being prepared. However, issues around temperature variations across the sample were observed during the curing process. As a result, the degree of cure across the DEC samples was 6–36 % lower than samples cured in a conventional oven. There is a pressing need to optimise the electrode configuration to improve the degree of cure and the final quality of the part.

In CFRP samples with a woven fabric, the resistivity along the fibre, R_{11} and R_{22} directions are low (0.022 m Ω ·m), while through the ply stack, R_{33} , the resistance is much higher (310 m Ω ·m) [28,29]. Thus, most electrical curing passes current along the carbon fibres. While the carbon fibre has a low resistance, the matrix is generally an insulator. Epoxy resins are insulators with breakdown electric fields of the order of 400 V/mm [30]. Thus, conduction through the ply stack is limited. This requires complex arrangements for the contacts, with many authors interdigitating numerous copper sheets at the edges. Ply drop can also be an issue as the high resistance at the end of the ply leads to uneven temperature distribution. In an effort to address these issues and decrease the resistivity of the epoxy resin, we added conductive, lowcost, carbon black (CB) nanoparticles to the epoxy resin. This results in a matrix (CB/epoxy resin nanocomposite) whose resistivity is less than 0.1 Ω ·m [31]. Even low concentrations, (0.1-3 wt%) of conductive nanoparticles significantly increase the conductivity of epoxy resins [32,33,34]. Thus, carbon nanoparticles offer a cost-effective method to address some of the limitations of DEC.

Carbon in the form of nanotubes (CNT) and graphene has been used to improve the conductivity of polymers and resins previously [35,36,37,38]. However, the dispersion of CNT and graphene in epoxy resin is difficult and time-consuming. Even small concentrations of well-dispersed CNTs and graphene lead to large increases in viscosity [36,37]. The tendency for these nanomaterials to aggregate leads to poor dispersion. This creates weaknesses and stress raisers that degrade the mechanical properties [39,40]. Importantly, for any prospective commercial venture, the cost of CB is considerably lower than CNTs or graphene.

In most DEC manufacturing processes [8,23,24], the current typically flows along the fibre direction. However, the contact area of the copper sheets at the edges of the samples is limited, and the matrix of CFRP is epoxy resin, which acts as an insulator. Consequently, the temperature distribution and energy consumption are suboptimal. To address these issues, this project proposes the incorporation of CB

conductive nanoparticles into the matrix and the implementation of a novel contact arrangement, known as the Top-Bottom mode, where the current flows perpendicular to the sample. As a result, this project compared unmodified CFRP cured by DEC with three different concentrations of CB in the matrix (1 wt%, 2 wt%, 3 wt%). The influence of CB on the electrical and mechanical properties is examined. Then, 2 wt% CB-modified epoxy resin, identified as the optimum concentration, in terms of flexural strength, is used to explore DEC. Four different electrode configurations were compared in terms of resistance and the distribution of temperature. This work represents a significant advancement in the power efficiency of composite manufacture through the use of nanoparticle conductive fillers in the matrix coupled with through ply electrical current to produce uniform CFRP samples.

2. Materials

· Epoxy resin system

The epoxy resin used in this work is IN2 epoxy infusion resin (Easy Composite, UK). This is a DEGBA-based low-viscosity resin. The low viscosity assists in the dispersion of the nanoparticles and subsequent infiltration of the fabric during hand layup. The hardener in this work is "AT30 slow" (AT30) from Easy Composites, this is a polymeric anime, that is a low-viscosity liquid at room temperature. For the cured IN2/AT30S resin, the density is 1.15 g/cm³.

• Carbon black (CB)

The carbon black (CB) in this work is "Carbon black, acetylene, 100 % compressed" from Alfa Aesar Ltd, and the density of CB is 2.1 g/cm³. According to the supplier's literature, the conductivity of this CB is 558 S/m.

• Carbon fibre

The carbon fibre used is "210g 2x2 Twill 3k Carbon Fibre Cloth" (Pyrofil TR30S 3 k Mitsubishi, supplied by Easy Composites) with a $0.021~{\rm g/cm^2}$ areal density and $1.79~{\rm g/cm^3}$ density (supplier's data).

3. Methodology

The relevant information concerning the equipment and techniques employed are summarised in this section.

3.1. Matrix modification and prepreg composite

This subsection includes three parts to describe the manufacturing process of CFRP with different concentrations of CB in the matrix. The first is the modification of the matrix with carbon black, then the hand layup procedure and finally the curing process.

3.1.1. Matrix modification

The CB particles were incorporated into IN2 resin at 0, 1, 2, and 3 wt % of the final epoxy matrix. Firstly, 100 g IN2 resin and the corresponding amount of CB were pre-mixed in a disposable plastic beaker by a wooden stirrer for 30 s. Then an overhead stirrer ("Hei-TORQUE Value 100" from Heidolph Instruments (Schwabach, Germany)), fitted with a four-blade mixing propeller stirrer, mixed the mixture for 10 min at 900 rpm. Subsequently, 30g of AT30 slow hardener, (30 wt% of final resin) was added to the mixture and mixed by the overhead stirrer for 3 min at 900 rpm. The final mixture was degassed under a vacuum before hand layup.

3.1.2. Prepreg composite manufacturing-hand layup

First, CR1 Easy-Lease Chemical Release Agent (Easy Composites) was sprayed on the glass mould surface to prevent adhesion. Then, 120*120

mm carbon fibre was placed on the glass surface. The degassed uncured polymer liquid was uniformly spread on the carbon fibre surface by brush. The last two steps were repeated until 15 layers of carbon fibre were stacked. 130*130 mm release film and vacuum breather were placed on the sample. Finally, the whole mould was covered with a vacuum bag and sealed with vacuum tape. The sample was degassed by a vacuum pump for 15 h at room temperature and de-mould to create "prepreg" samples. This process was intended to increase the reproducibility of the hand layup, in terms of fibre volume fraction and resin distribution.

3.2. Composite manufacturing

Here four different manufacturing methods are discussed, three traditional, heated press, autoclave, and oven; and DEC with four different electrode configurations.

3.2.1. Heated press

The heated press used is Moore Hydraulic Heated Platen Press (George E Moore & Son Ltd, UK), which provides 20 tons maximum load. The platens were closed to a gap of 4 mm, and a pressure of 2.1 MPa was applied. The sample was heated at a rate of 3 $^{\circ}$ C/min to 70 $^{\circ}$ C. This was held for 3 h.

3.2.2. Autoclave

An AC052 Autoclave (Premier Autoclaves Service and Solutions, UK) was used to cure the composite panel using a 3 $^{\circ}$ C/min ramp to 70 $^{\circ}$ C for 3 h. The autoclave pressure was set to 6 bar gauge, with the sample bag under vacuum at all times. This results in a consolidation pressure of 7 bar absolute or 0.7 MPa.

3.2.3. Oven

A UT 6200 electric lab oven (Thermo Fisher Scientific Inc. Waltham, USA) was used. A heating ramp of 3 °C/min used to heat from room temperature to 70 °C. The temperature was held at 70 °C for 3 h. An external vacuum pump was used to set a vacuum of -0.8 bar gauge (200 mbar absolute) or 0.08 MPa.

3.2.4. Direct electric cure, DEC

A PS1540S SMPS, bench power supply (Rapid Electronics, UK), provided DC electrical power for DEC. The voltage of the power supply is manually controlled between 10 and 15 V to maintain the sample temperature between 60–70 °C. The hydraulic press (section 3.2.2.1) was used to compress prepreg at 2.1 MPa during DEC.

To examine the influence of contact arrangement with the conductive resin during DEC, four contact configurations were examined. The copper sheets were inserted to a depth of 1 cm to create contact with the samples. Cables provide electrical contact to the copper sheets from the power supply. Fig. 1 shows the schematic of the different electrode contact arrangements and the positive and negative electrodes of the power supply.

3.3. Experimental testing and analysis

3.3.1. Resistance changes during the DEC process

The voltage and current display screens of the bench power supply were used to calculate the resistance of the specimens. Due to their low resistivity, the influence of electrical cables was ignored.

3.3.2. Temperature distribution during the DEC process

Seven thermocouples (centre of the top surface, centre of the bottom surface, and five in the middle layer Fig. 2) were used to record temperature change versus time by a USB TC-08 thermocouple data logger (Pico Technology, UK).

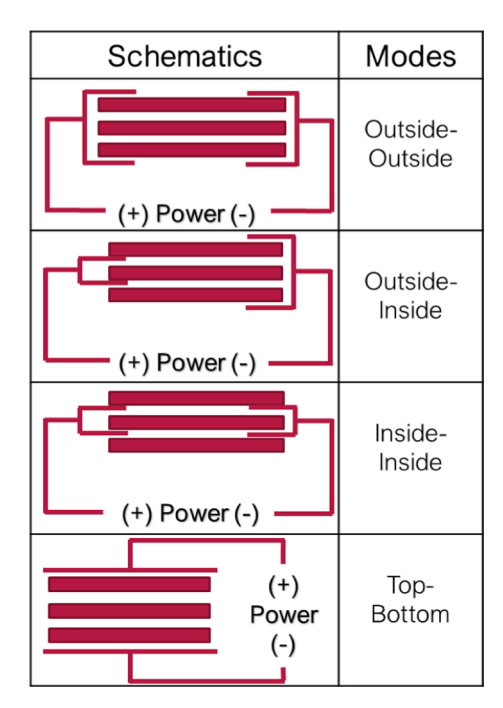


Fig. 1. The schematic of different contact arrangements in DEC manufacturing (one red bar in the schematic is 5 layers of carbon fibre and conductive resin). The gaps between the layers are not present in the samples, they are shown to aid clarity in the positioning of the electrodes. The thin red lines are copper sheets and copper wires).

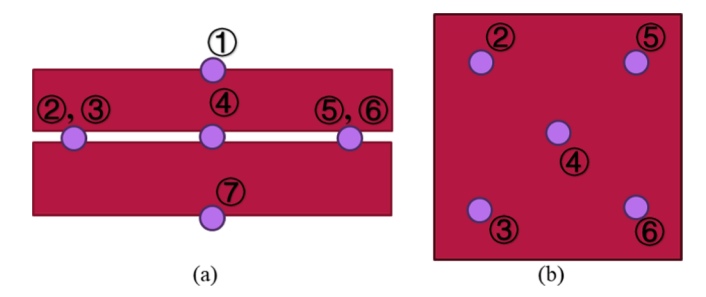


Fig. 2. The schematic of thermocouples distribution in samples at (a) middle cross-section (b) middle layer (the thin and thick red bars are 7 layers and 8 layers laminate respectively, and purple circles are thermocouples (1-top centre, 2,3-left middle, 4-centre middle, 5,6-right middle, 7-bottom middle)).

3.3.3. Flexural tests

The 4-point flexural tests were conducted on an H5KS Benchtop Tester from Tinius Olsen (Horsham, USA) with a 1 mm/min crosshead speed. The test specimen dimension and testing conditions were determined by ASTM D7264 Standard. The dimension of the specimens was $80\times14\times4$ mm (L \times W \times T). The thickness varies due to the different CB concentrations and manufacturing methods.

3.3.4. Degree of cure (DoC)

DSC was used to determine the degree of cure (DSC Q20, TA Instruments, New Castle, USA) [41]. The DSC was heated from 40 $^{\circ}$ C to 250 $^{\circ}$ C with a 10 $^{\circ}$ C/min ramp.

3.3.5. The energy consumption of curing process calculation

A Power Meter (Intertek, UK) was used to record the energy consumption during the curing process in the DEC, heat press and oven curing. The energy consumption of the AC052 Autoclave is measured by a 3-phase in-line power meter (model RI-70–100-P, Rayleigh Instruments, UK).

4. Result and discussion

4.1. Flexural properties

CFRP with different CB concentrations (0, 1, 2 and 3 wt%) in the matrix was manufactured by the heated press. The flexural strengths and flexural moduli of these CFRP samples were determined by 4-point bending. The data is presented in Fig. 3. As the CB concentration increases, the flexural strength increases. At 2 wt%, the flexural strength reaches a maximum, 730 ± 12.8 MPa. Compared with unmodified CFRP (0 wt%), this is an increase of 31 %. At 3 wt% CB, the flexural strength decreases slightly. At higher nanoparticle concentrations, nanoparticles may aggregate and these act as stress risers, which degrade the properties of the CFRP [39,42,43]. While it is difficult to compare across different carbon fibre fabrics, these results compare well with Haves et al. who achieved 800 MPa and 48 GPa for flexural strength and modulus respectively, for Cycom 950-1 plain weave pre-preg. They see very similar values for autoclave, oven and DEC [24]. Likewise, as can be seen from Fig. 3, there is no statistically significant variation in flexural modulus across the series. An ANOVA p-value of 2.065 was determined. This is lower than the critical F-statistic of 3.06 for an α of 0.05. While there is a significant difference in flexural strength. This implies that even though the CB particles are expected to have a higher stiffness than the IN2/AT30S resin, the low concentration means they do not impede the compression of the resin and thus have no effect on the flexural modulus. However, the CB nanoparticles do impede failure in the system. Nanoparticles are known to prevent crack growth by a variety of mechanisms. This has also been widely reported in the literature [44,45,46,47,48]. As the 2 wt% sample shows the highest strength this concentration was chosen for further DEC analysis. Table 1 shows the physical properties of samples. The DoC of all samples is high than 98 %.

4.2. Comparative DEC study of CFRP with 2 wt% CB

Preliminary trails, via resistance measurements were undertaken that showed a percolation limit of around 2–3 %. In addition, the four-point bending test shows CFRP has the best mechanical properties when CB is 2 wt% in the matrix. As a result, CFRP with 2 wt% is used to examine the DEC manufacturing methods. Table 2 shows the physical properties of the 2 wt% CB-CFRP sample, cured by DEC, autoclave, hot pressing and oven. When comparing various curing strategies, it is noted that the oven cure applies a consolidating pressure of 1 bar (0.1 MPa), while the autoclave exerts a pressure of 7 bars (0.7 MPa), and the heat press can achieve up to 2 MPa. Under increased pressure, a greater amount of uncured resin is expelled from the samples. This results in

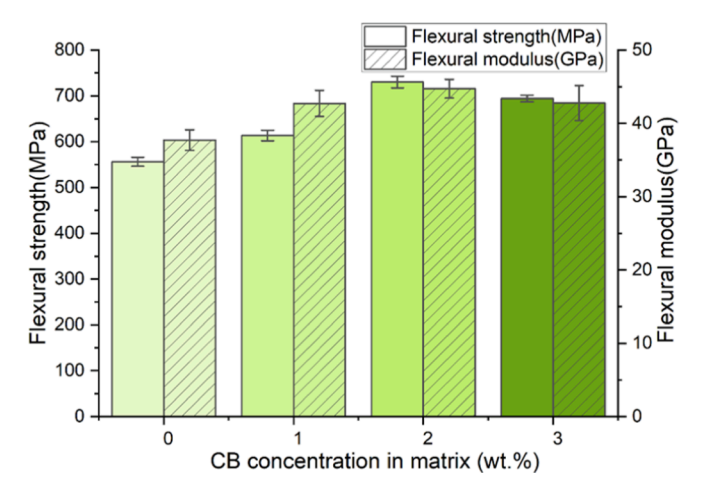


Fig. 3. The flexural strength and modulus of the CFRP with different CB wt.%. The error bar is the standard deviation of 5 samples.

Table 1The physical properties of the CFRP samples with different CB wt.% in matrix; the error is the standard deviation of three samples.

CB concentration in matrix (wt.%)	Density ¹ (g/cm ³)	Fibre volume fraction (vol. %)	Fibre mass fraction (wt. %)	Void fraction ² (wt.%)
0	$1.4635 \pm \\ 0.0049$	51.26 ± 0.74	62.70 ± 0.69	3.06 ± 0.72
1	$\begin{array}{c} 1.4802 \pm \\ 0.0039 \end{array}$	53.47 ± 0.59	64.66 ± 0.54	2.94 ± 0.23
2	$\begin{array}{c} \textbf{1.4407} \; \pm \\ \textbf{0.0009} \end{array}$	49.47 ± 0.13	$\begin{array}{c} 60.83 \pm \\ 0.13 \end{array}$	2.69 ± 0.52
3	$\begin{array}{c} \textbf{1.4488} \; \pm \\ \textbf{0.0026} \end{array}$	48.56 ± 0.40	$59.87\ \pm$ 0.38	4.84 ± 0.24

Table 2The physical properties of the CFRP samples manufactured by different methods; the error is the standard deviation of three samples.

Curing	Density ¹ (g/cm ³)	Fibre volume fraction (vol.%)	Fibre mass fraction (wt.%)	Thickness (mm)	Void fraction ² (wt.%)
DEC- Inside- Inside	$1.4219 \pm \\ 0.0016$	$44.36 \pm \\ 0.24$	55.84 ± 0.24	4.22 ± 0.02	1.54 ± 0.17
DEC- Inside- Outside	1.4225 ± 0.0009	$44.44 \pm \\ 0.14$	55.92 ± 0.14	$\begin{array}{l} \textbf{4.38} \pm \\ \textbf{0.02} \end{array}$	$\begin{array}{l} 3.53 \pm \\ 0.27 \end{array}$
DEC- Outside- Outside	$\begin{array}{c} \textbf{1.4407} \pm \\ \textbf{0.0079} \end{array}$	$47.20 \pm \\1.20$	$58.63 \pm \\1.18$	$\begin{array}{l} 4.18 \pm \\ 0.04 \end{array}$	$\begin{array}{c} \textbf{3.24} \pm \\ \textbf{0.41} \end{array}$
DEC-Top- Bottom	$\begin{array}{c} 1.4488 \; \pm \\ 0.0014 \end{array}$	$48.41\ \pm$ 0.22	$\begin{array}{c} 59.82 \pm \\ 0.21 \end{array}$	$\begin{array}{c} \textbf{3.87} \pm \\ \textbf{0.12} \end{array}$	$\begin{array}{c} 5.09 \pm \\ 0.12 \end{array}$
Heated press	$1.4558 \pm \\ 0.0009$	$49.47 \pm \\ 0.14$	$\begin{array}{c} 60.83 \pm \\ 0.13 \end{array}$	3.73 ± 0.03	$\begin{array}{c} \textbf{2.69} \pm \\ \textbf{0.52} \end{array}$
Oven	$\begin{array}{c} {1.3967} \pm \\ {0.0125} \end{array}$	$40.54 \pm \\1.89$	$51.95 \pm \\1.96$	4.53 ± 0.05	$\begin{array}{c} \textbf{2.65} \; \pm \\ \textbf{0.41} \end{array}$
Autoclave	$\begin{array}{c} 1.4077 \; \pm \\ 0.0030 \end{array}$	42.20 ± 0.45	$53.67 \pm \\ 0.46$	$\begin{array}{c} \textbf{4.48} \pm \\ \textbf{0.07} \end{array}$	$\begin{array}{c} \textbf{1.47} \pm \\ \textbf{0.19} \end{array}$

 $^{^{\}rm 1}$ As determined by Helium pycnometry. $^{\rm 2}\! {\rm Determined}$ from helium and density balance data.

thinner samples and higher fibre volume fractions, see, see Fig. 4. Although the mass of fibre remains constant across all samples, the fibre fraction varies. However, due to the high viscosity of the prepreg, the variation in fibre fraction induced by different pressures remains within

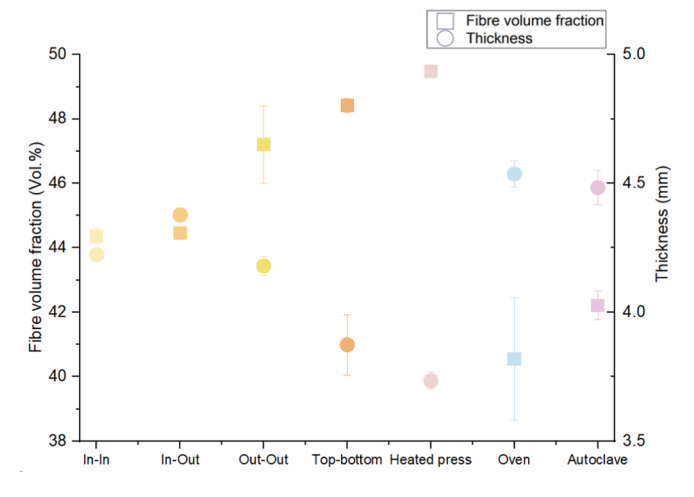


Fig. 4. The volume fraction of fibre and sample thickness in different manufacturing methods (the value is the average of 3 samples and the error bar is the standard deviation.

f Determined from helium and density balance data

acceptable limits. In terms of direct comparisons, the maximum difference in the fibre volume fraction is less than 10 %. In addition, in all the curing methods, the measured void fraction of the sample is lower than 6 %. The particle density calculated by helium pycnometry machine is reliable. However, the bulk density calculated by density balance could be lower than real value. Because when put the sample in the water in density balance, there are some air bubbles around the sample, which increases the volume of sample in calculation. As a result, the calculated void fraction should be regarded as a higher limitation.

Y. Tang and J. Patrick A. Fairclough

In terms of DEC methods, the void fraction of Top-Bottom is higher than others. There are probably two reasons for this, firstly, to facilitate the insertion of copper sheet for the Inside-Inside and Inside-Outside modes, three laminates (each of 5 plies of carbon fibre) were initially prepared by hand layup. The method to do this was to have one ply of carbon fibre on the glass, resin with CB was applied on the top by hand using a brush, and the next ply was placed on top of this. In this way a stack of 5 plies was created, these were then vacuum consolidated. These were left overnight under a vacuum. In the morning, the vacuum was released, and the copper contacts were inserted. Then, the assembly was then consolidated in the (unheated) press at 2 MPa and cured. However, in terms of Top-Bottom, only one prepreg laminate, of 15 plies was created, left under vacuum overnight, and contacts were added. It was then (unheated) press consolidated and cured. The separate 5-layer stack resulted in a lower void fraction. Secondly, the curing temperature of Top-Bottom was a little lower than other DEC methods (70°C vs 80°C, see Fig. 5). In the initial stage of curing, as the temperature increases, the viscosity of resin will decrease, this improves impregnation reducing the void content.

4.3. The resistance of 2 wt% CB-CFRP during the DEC process

The resistivity of CFRP with 2 wt% is 70 % that of unmodified CFRP. Fig. 5 shows the resistance of a 2 wt% CB-CFRP with time for the four DEC curing configurations. During the initial curing process, the resistance drops as the sample temperature increases. Due to the manual control and the rapid heating response created by small adjustments to the current, the rate of temperature rise was limited to approximately $0.5\,^{\circ}\text{C/min}$. This is lower than that in traditional curing methods but can be increased with automated control systems. In this process, the resin is heated by Joule heating and its viscosity initially decreases as temperature rises. This lower viscosity allows the CB particles to diffuse faster. Meanwhile, the polymerization of resin leads to reaction-induced phase separation (RIPS). In this process, CB nanoparticles form networks that reduce the resistance of the system. When the cure time reaches 75 min, the temperature has increased to around 60 °C and the resistance starts to plateau. At this point, the degree of polymerization is high, consequently, the viscosity is high, and the movement of CB nanoparticles is slowed. This plateau in resistance is a clear indication that curing is almost complete.

RIPS is commonly observed in polyurethanes, polymer blends and solutions [49]. However, phase separation is a basic consequence of the reduced configurational entropy of the polymer compared to the monomer, and is thus a universal phenomenon [50,51,52]. Several authors have shown that phase separation in polymer-nanoparticle systems is a common occurrence [53,54,55].

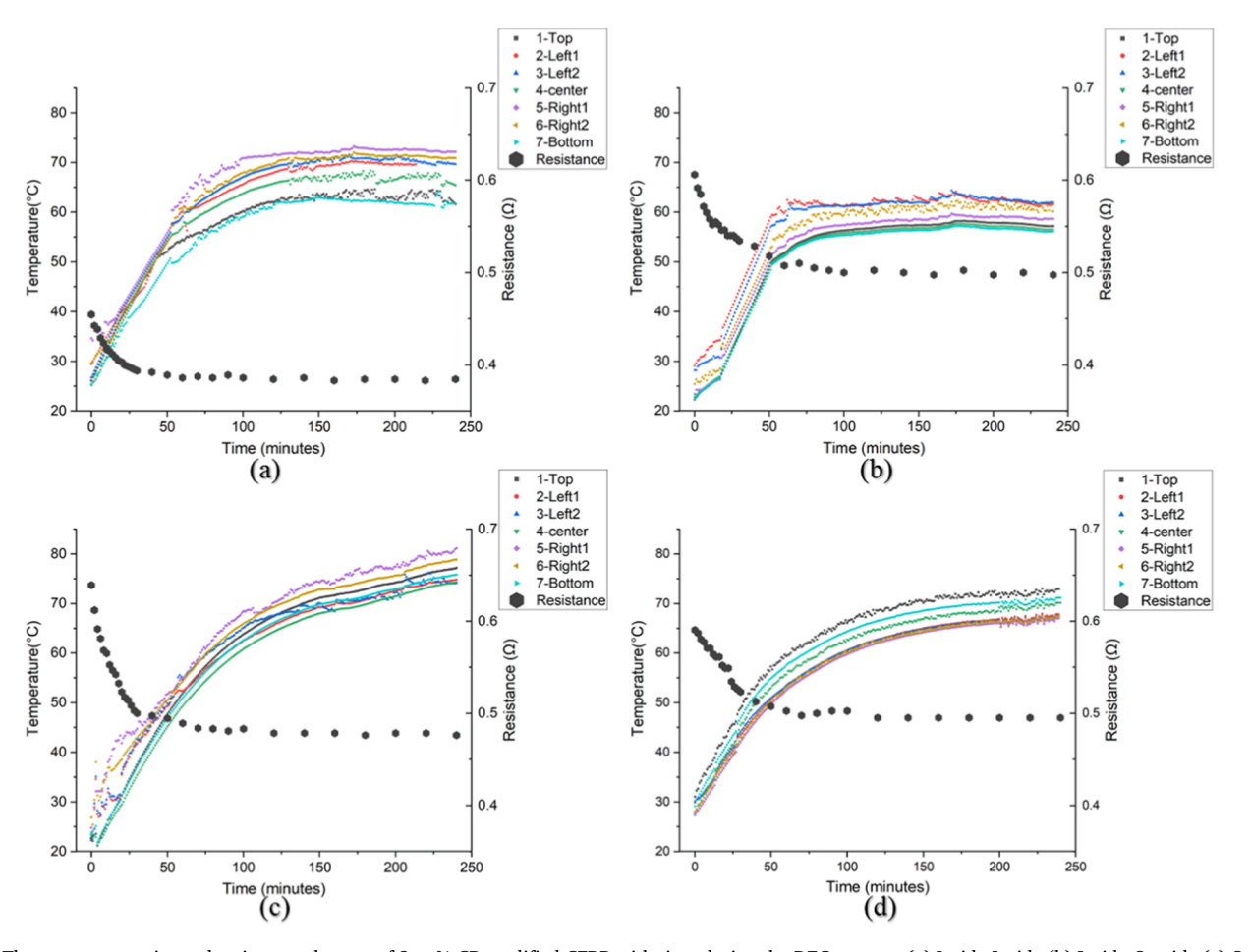


Fig. 5. The temperature rise and resistance changes of 2 wt% CB modified CFRP with time during the DEC process. (a) Inside-Inside (b) Inside-Outside (c) Outside-Outside (d) Top-Bottom.

4.4. The temperature distributions during the DEC process

Collinson *et al.* [8] used DEC with an outside-outside configuration to cure CFRP prepreg. They report temperature differences of 11 °C, which is a little higher than the 7 °C temperature difference reported here for the outside-outside configuration. They used a 3 k plain weave with a vacuum infusion system however they do not state the consolidation pressure. When the CFRP is cured without consolidation pressure, the maximum temperature difference is between 15 and 20°C [24]. Fig. 5 shows that the temperature differences within a sample are small, with a maximum difference of 10 °C, which occurs in the Inside-Inside mode. The minimum difference is in the Top-Bottom mode, a thought ply configuration, which is half of the maximum, circa. 5 °C. As a result, DEC manufacturing shows good temperature distribution during the curing process when CB is added at a low concentration.

In this project, the carbon fibre is twill weave fibre, which is an isotropic weave. As a result, the carbon fibre has the same electrical and thermal conductivity in the x and y direction. Therefore, in these two modes, the current always flows along the fibre direction. In addition, because of the isotropic property in thermal conductivity, the samples show good temperature distribution in the middle plane. The maximum temperature difference is lower than 5 $^{\circ}$ C.

The fibre direction plays an important part as the conductivity along the fibres is far higher than perpendicular to the fibres. One justification for adding CB is to create a more homogeneous resistance profile along, compared with perpendicular to, the fibres. Thus, there is less localised heating in the regions where different orientations are present. The use of woven fabric, 2x2 twill, intrinsically has a low resistance at 0 and 90. The use of CB reduces the difference in resistivity along and across the fibres. Our hypothesis is that this would allow for more uniform curing.

During the DEC process, the samples are placed in the unheated hot press and pressed by the two unheated steel plates, electrically insulated by thin PTFE sheets of 0.3 mm thickness. The heat loss is primarily via conduction through the PFTE film to the large steel plates. The Top-Bottom configuration places the electrical contacts immediately adjacent to the PTFE, this, coupled with the more uniform current distribution through the thickness of the sample results in the most uniform temperature distribution. However, even with this configuration the Top and Bottom temperatures are lower, due to heat conduction to the

platens.

In the Outside-Outside and Inside-Inside modes, the electrodes contact the two sides (left and right) of two carbon fibre plys, Outside-Outside and four plys in Inside-Inside modes. The current flows predominantly through these plys, due to the low resistance of the carbon fibre. In Outside-Inside mode, we surmise that the current must pass through the resin layers as the temperature distribution is similar to the Top-Bottom mode. This suggests that the current must flow along the carbon fibre and then through the bulk of the sample. The carbon fibre fabric at the top and bottom acts as distribution electrodes. In Top-Bottom mode, the current goes through the whole sample. The whole sample thickness generates Joule heating instead of a localised region. Thus, the temperature distribution in the Top-Bottom mode is improved over the other three modes.

Another general feature observed is that in all of the four DEC modes, the highest temperatures occur close to positive electrodes, followed by positions close to negative electrodes. The same effect is shown in the work of Collinson *et al.* [8] who also use DC current. Contact resistance at the copper-carbon interface plays the most significant role here. Additionally, the higher temperature of the positive electrode suggests that differences in electrochemical potential play a part. In essence, the positive electrode reverse biases the copper-carbon junction and thus generates more heat.

4.5. The DoC of CFRPs with 2 wt% CB in matrix

The degree of cure, DoC, of the 2 wt% CB-CFRPs is presented in Fig. 6. The traditional curing methods (autoclave, oven, and heat press) result in higher DoC than DEC. The CB-CFRPs by autoclave have the highest DoC (99 % in the centre and 98 % in the edge, as measured by DSC).

The differences between the DoC in the centre and edge of CFRPs manufactured by the more traditional curing methods are smaller than those manufactured by the DEC manufacturing method. However, the maximum difference in DoC between the centre and the edge is only 2 %, for the Inside-Inside sample. This configuration also has the lowest DoC of 90–92 %. The sample manufactured in Top-Bottom mode has the highest DoC values and the smallest difference between the centre and edge of 1 %. This compares favourably with the literature, Collinson

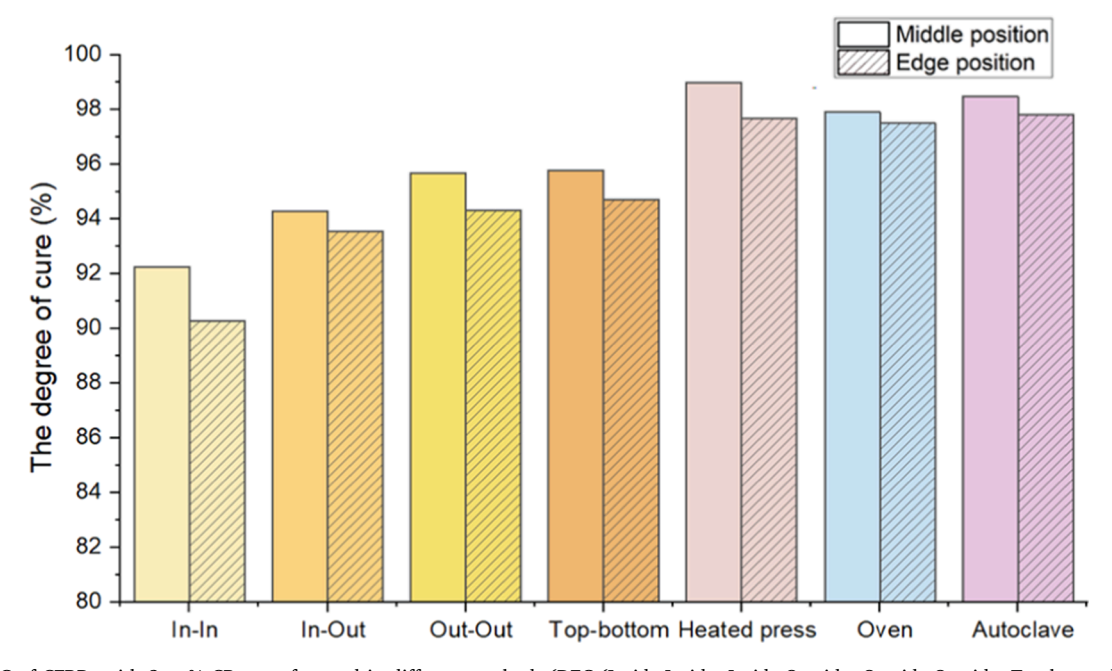


Fig. 6. The DOC of CFRPs with 2 wt% CB manufactured in different methods (DEC (Inside-Inside, Inside-Outside, Outside-Outside, Top-bottom) and traditional manufacturing methods (Autoclave, Oven, and Heat Press)).

et al. achieve a 35.4 % middle to edge difference [8,22,24].

While the addition of CB does not solve the issues around variations in the cure, it does improve the situation when coupled with the Top-Bottom and Outside-Outside configurations to a level comparable with conventional oven and autoclave methods.

4.6. Comparison of flexural testing for 2 wt% CB-CFRP

Fig. 7 shows the flexural properties of 2 wt% CB-CFRP with in the matrix. There is no statistically significant difference (by ANOVA) in the flexural strength or modulus of the CB-CFRP samples. For a level of significance, α , of 0.05, the F-statistics are 1.55 (strength) and 0.72 (modulus), and the critical F value is 2.69. As a result, CB-CFRPs manufactured by DEC have statistically the same flexural strength and modulus as the traditional curing methods. It should be noted that both the oven and the autoclave samples were slightly thicker than the heated press and DEC samples, (Fig. 4 and.

Table 1). Similar comparisons in the literature between DEC and conventional curing methods also show that DEC is equivalent to conventional curing methods in terms of flexural properties. [24,56,57].

4.7. Energy consumption

Table 3 shows the total energy consumption for the curing processes. Our energy consumption testing demonstrated a 90 % energy reduction in DEC compared to the autoclave, which is the highest at 10.03 kW•h with no significant effect on mechanical properties. For the four DEC modes, Outside-Outside and Top-Bottom modes show the lowest energy consumption. The energy volume density in these two modes is about 68 % of that in the Inside-Inside mode. The Inside-Inside mode shows a faster temperature rise and a longer high-temperature region, the widest variation in temperature and the lowest DoC. The uneven temperature distribution, due to the relatively poor thermal conduction perpendicular to the carbon fibres and the presence of the unheated steel plates of the press results in this poor temperature distribution. Thus, for DEC, insulation of the part as well as electrode placement, avoiding the Inside-Inside configuration needs to be more carefully considered.

The energy consumption between DEC and heat press manufacturing methods is not significantly different. There are two primary reasons for this. Firstly, in the case of DEC samples, an unheated hot press was used to provide consolidation. However, there was insufficient insulation

between the sample and the press, with only a thin Teflon film on the sample surface. Consequently, the plates became warm to the touch, leading to higher energy consumption for the DEC method. The better insulation materials should be considered in the future work. Secondly, the cross-sectional area of the sample is about 50 % of the heat press platform, whereas, in the oven and autoclave processes, the sample volume occupies less than 1 % of the available space. Therefore, with smaller sample sizes, the energy consumption advantage of DEC manufacturing becomes more pronounced. In summary, DEC manufacturing demonstrates good performance for small-size products.

Comparisons with literature are difficult due to the lack of sample data, most authors do not give either the power consumed, the sample mass, density nor the dimensions of the sample. The thickness often needs to be estimated based on the fibre count and weave. However, but this can vary considerably (20–30 %) due to the different resin chemistries, viscosities and consolidation pressures. However, Liu et al. have an energy consumption of 475 J/mm³ [58], for their non-insulated DEC carbon repair system; Lee et al. 19 J/mm³ [22] for their carbon nanotube heating mat arrangement with insulation. Assuming a carbon fibre thickness of 2 x 2 mm on each side of the Nomex, Collinson et al. consume 12 J/mm³ [8]. Table 3 details the energy density required to cure the samples in the various configurations to allow a meaningful comparison amongst the different methods and with the literature.

Table 3The energy consumption of the curing process in different manufacturing methods.

Curing	Total energy consumption (MJ)	Average power (Kw)	Energy volume density (J/mm ³)
DEC-Inside- Inside	5.31	0.37	87.32
DEC-Inside- Outside	3.79	0.26	60.10
DEC-Outside- Outside	3.01	0.21	49.94
DEC-Top- Bottom	3.16	0.22	56.65
Heated press	3.68	0.34	68.57
Oven	9.50	0.88	145.70
Autoclave	36.07	3.34	559.15

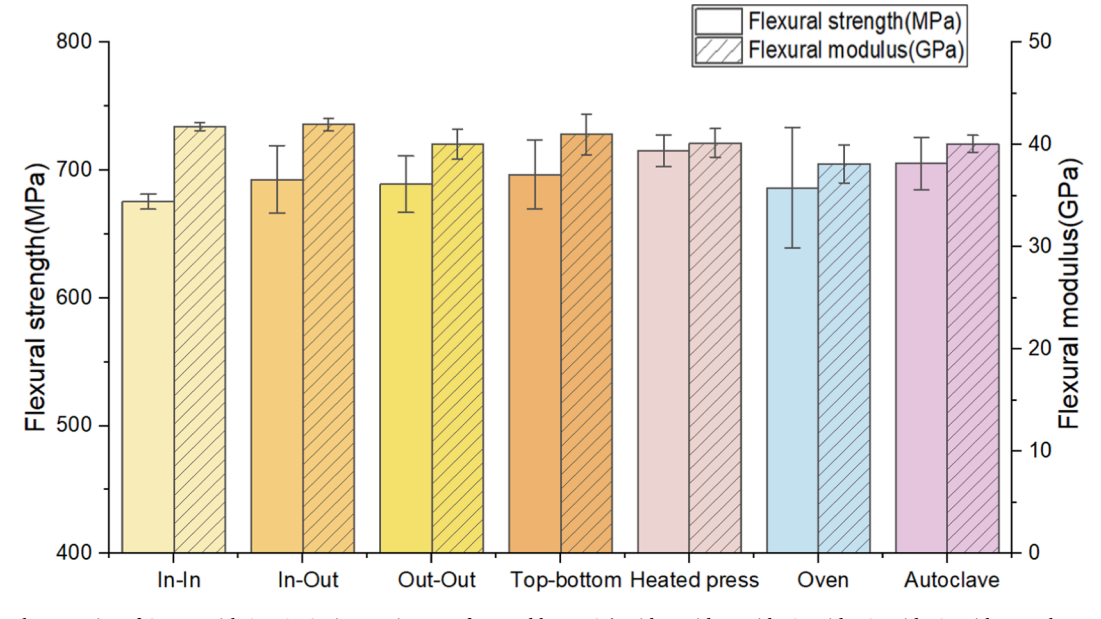


Fig. 7. The flexural properties of CFRPs with 2 wt% CB in matrix manufactured by DEC (Inside-Inside, Inside-Outside, Outside, Outside, Top-bottom) and traditional manufacturing methods (Autoclave, Oven, and Heat Press). The average value is from 5 samples and the error bar is the standard deviation of samples.

5. Conclusions

Direct electrical cure, DEC, is a cost-effective and viable option for the low-energy cure of carbon fibre-reinforced polymer, CFRP, components. We show a 12-fold reduction in energy consumption compared with autoclave cure. DEC requires minimal capital investment, further removing barriers for small enterprises to produce CFRP parts. The inclusion of 2 wt% carbon black, CB, creating a conductive epoxy matrix, additionally improves the flexural strength of the component. This addition of CB and external pressure provided by an unheated press, improves the temperature distribution, the final degree of cure and uniformity of cure, across a wide range of DEC contact modes. When electrical current flows perpendicular to the plys, as opposed to along them, DEC shows excellent performance in terms of fibre volume fraction, temperature uniformity and the degree of cure.

CRediT authorship contribution statement

Yunlong Tang: Writing – original draft, Visualization, Validation, Software, Methodology, Formal analysis, Data curation. **J. Patrick A. Fairclough:** Writing – original draft, Writing – review & editing, Supervision, Project administration, Funding acquisition.

Declaration of competing interest

The authors declare that they have no known competing financial interests or personal relationships that could have appeared to influence the work reported in this paper.

Data availability

Data will be made available on request.

Acknowledgements

Thanks go to Dr Chris Holland and Dr Andrew Parnell for assistance with writing guidance.

Data availability.

Data will be made available on request.

Funding statement

Some of the equipment used in this work was funded through an Engineering and Physical Sciences Research Council grant (EPSRC) Grant number EP/R041733/1.

References

- Barile C, Casavola C, De Cillis F. Mechanical comparison of new composite materials for aerospace applications. Compos B Eng Apr. 2019;162:122–8. https://doi.org/10.1016/j.compositesb.2018.10.101.
- [2] J. Skoczylas, S. Samborski, and M. Klonica, 'The application of composite materials in the aerospace industry', *J Technol Exploit Mech Eng*, vol. 5, no. 1, Jan. 2019, 10.35784/jteme.73.
- [3] M. Słowiński, 'An Analysis of CFRP Application in the Construction of Rail Vehicles', Problemy Kolejnictwa - Railway Reports, vol. 65, no. 193, pp. 105–113, Dec. 2021, 10.36137/1935E.
- [4] Zhang J, Lin G, Vaidya U, Wang H. Past, present and future prospective of global carbon fibre composite developments and applications. Compos B Eng Feb. 2023; 250:110463. https://doi.org/10.1016/J.COMPOSITESB.2022.110463.
- [5] Drakonakis VM, Seferis JC, Doumanidis CC. Curing Pressure Influence of Out-of-Autoclave Processing on Structural Composites for Commercial Aviation. Adv Mater Sci Eng 2013;2013:1–14. https://doi.org/10.1155/2013/356824.
- [6] Yoshida H, Ogasa T, Hayashi R. Statistical approach to the relationship between ILSS and void content of CFRP. Compos Sci Technol Jan. 1986;25(1):3–18. https://doi.org/10.1016/0266-3538(86)90018-7.
- [7] Vijayan DS, Sivasuriyan A, Devarajan P, Stefańska A, Wodzyński Ł, Koda E. Carbon Fibre-Reinforced Polymer (CFRP) Composites in Civil Engineering Application—A Comprehensive Review. Buildings Jun. 2023;13(6):1509. https://doi.org/ 10.3390/buildings13061509.
- [8] Collinson MG, Swait TJ, Bower MP, Nuhiji B, Hayes SA. Development and implementation of direct electric cure of plain weave CFRP composites for aerospace. Compos Part A Appl Sci Manuf Sep. 2023;172:107615. https://doi.org/ 10.1016/j.compositesa.2023.107615.

- [9] Chowdhury IR, Summerscales J. Cool-Clave—An Energy Efficient Autoclave. Journal of Composites Science Feb. 2023;7(2):82. https://doi.org/10.3390/ier70.20082
- [10] Keller A, Dransfeld C, Masania K. Flow and heat transfer during compression resin transfer moulding of highly reactive epoxies. Compos B Eng Nov. 2018;153: 167–75. https://doi.org/10.1016/j.compositesb.2018.07.041.
- [11] Abliz D, Duan Y, Steuernagel L, Xie L, Li D, Ziegmann G. Curing Methods for Advanced Polymer Composites - A Review. Polym Polym Compos Jul. 2013;21(6): 341–8. https://doi.org/10.1177/096739111302100602.
- [12] Ramulu M, Stickler PB, McDevitt NS, Datar IP, Kim D, Jenkins MG. Influence of processing methods on the tensile and flexure properties of high temperature composites. Compos Sci Technol Sep. 2004;64(12):1763–72. https://doi.org/ 10.1016/j.compscitech.2003.12.008.
- [13] Papargyris DA, Day RJ, Nesbitt A, Bakavos D. Comparison of the mechanical and physical properties of a carbon fibre epoxy composite manufactured by resin transfer moulding using conventional and microwave heating. Compos Sci Technol Jun. 2008;68(7–8):1854–61. https://doi.org/10.1016/j.compscitech.2008.01.010.
- [14] Rao S, Rao R. Cure studies on bifunctional epoxy matrices using a domestic microwave oven. Polym Test Aug. 2008;27(5):645–52. https://doi.org/10.1016/j. polymertesting.2008.04.005.
- [15] Li N, Li Y, Hang X, Gao J. Analysis and optimization of temperature distribution in carbon fiber reinforced composite materials during microwave curing process. J Mater Process Technol Mar. 2014;214(3):544–50. https://doi.org/10.1016/j. jmatprotec.2013.10.012.
- [16] Li S, Li Y, Zhou J, Wen Y. Improvement of Heating Uniformity by Limiting the Absorption of Hot Areas in Microwave Processing of CFRP Composites. Materials Dec. 2021;14(24):7769. https://doi.org/10.3390/ma14247769.
- [17] Zhilyaev I, Brauner C, Queloz S, Jordi H, Lüscher R, Conti S, et al. Controlled curing of thermoset composite components using infrared radiation and mathematical modelling. Compos Struct Mar. 2021;259:113224. https://doi.org/ 10.1016/j.compstruct.2020.113224.
- [18] Kumar PK, Raghavendra NV, Sridhara BK. Optimization of infrared radiation cure process parameters for glass fiber reinforced polymer composites. Mater Des Mar. 2011;32(3):1129–37. https://doi.org/10.1016/j.matdes.2010.11.001.
- [19] Rudnev V, Loveless D, Cook RL, Black M. Handbook of Induction Heating. Handbook of Induction Heating Dec. 2002. https://doi.org/10.1201/ 9781420028904.
- [20] Ambrell Corporation, '5 BASICS OF INDUCTION HEATING COIL DESIGN'. Accessed: Aug. 08, 2023. [Online]. Available: https://www.ambrell.com/blog/5-basics-of-induction-heating-coil-design.
- [21] Mgbemena CO, Li D, Lin M-F, Liddel PD, Katnam KB, Thakur VK, et al. Accelerated microwave curing of fibre-reinforced thermoset polymer composites for structural applications: A review of scientific challenges. Compos Part A Appl Sci Manuf Dec. 2018;115:88–103. https://doi.org/10.1016/j.compositesa.2018.09.012.
- [22] Lee J, Ni X, Daso F, Xiao X, King D, Gómez JS, et al. Advanced carbon fiber composite out-of-autoclave laminate manufacture via nanostructured out-of-oven conductive curing. Compos Sci Technol Sep. 2018;166:150–9. https://doi.org/ 10.1016/j.compscitech.2018.02.031.
- [23] Fukuda H. Processing of carbon fiber reinforced plastics by means of Joule heating. Adv Compos Mater Jan. 1994;3(3):153–61. https://doi.org/10.1163/ 1565510470015
- [24] Hayes SA, Lafferty AD, Altinkurt G, Wilson PR, Collinson M, Duchene P. Direct electrical cure of carbon fiber composites. Adv Manuf Polym Compos Sci Apr. 2015;1(2):112–9. https://doi.org/10.1179/2055035915Y.0000000001.
- [25] Joseph C, Viney C. Electrical resistance curing of carbon-fibre/epoxy composites. Compos Sci Technol Feb. 2000;60(2):315–9. https://doi.org/10.1016/S0266-3538 (99)00112-8.
- [26] Chien A-T, Cho S, Joshi Y, Kumar S. Electrical conductivity and Joule heating of polyacrylonitrile/carbon nanotube composite fibers. Polymer (Guildf) Dec. 2014; 55(26):6896–905. https://doi.org/10.1016/j.polymer.2014.10.064.
- [27] Çelik M, Noble T, Haseeb A, Maguire J, Robert C, Brádaigh CMÓ. Contact resistance heating of unidirectional carbon fibre tows in a powder-epoxy towpregging line. Plast, Rubber Compos Sep. 2022;51(8):383–92. https://doi.org/ 10.1080/14658011.2022.2108982.
- [28] Irving PE, Thiagarajan C. Fatigue damage characterization in carbon fibre composite materials using an electrical potential technique. Smart Mater Struct Aug. 1998;7(4):456–66. https://doi.org/10.1088/0964-1726/7/4/004.
- [29] Todoroki A, Tanaka M, Shimamura Y. Measurement of orthotropic electric conductance of CFRP laminates and analysis of the effect on delamination monitoring with an electric resistance change method. Compos Sci Technol Apr. 2002;62(5):619–28. https://doi.org/10.1016/S0266-3538(02)00019-2.
- [30] T. Dakin, 'Application of Epoxy Resins in Electrical Apparatus', *IEEE Transactions on Electrical Insulation*, vol. EI-9, no. 4, pp. 121–128, Dec. 1974, 10.1109/TEI.1974.299321.
- [31] Kupke M, Wentzel H-P, Schulte K. Electrically conductive glass fibre reinforced epoxy resin. Mater Res Innov Nov. 1998;2(3):164–9. https://doi.org/10.1007/ s100190050079
- [32] Wang Y, Weng GJ. Electrical Conductivity of Carbon Nanotube- and Graphene-Based Nanocomposites. In: Micromechanics and Nanomechanics of Composite Solids. Cham: Springer International Publishing; 2018. p. 123–56. https://doi.org. 10.1007/978-3-319-52794-9
- [33] Liu Y, Lu J, Cui Y. Improved thermal conductivity of epoxy resin by graphene–nickel three-dimensional filler. Carbon Resources Conversion Jan. 2020; 3:29–35. https://doi.org/10.1016/j.crcon.2019.12.003.
- [34] Buketov A, Smetankin S, Lysenkov E, Yurenin K, Akimov O, Yakushchenko S, et al. Electrophysical Properties of Epoxy Composite Materials Filled with Carbon Black

- Nanopowder. Adv Mater Sci Eng 2020;2020. https://doi.org/10.1155/2020/6361485
- [35] Blokhin A, Zaytsev I, Sukhorukov A, Stolyarov R, Popov A, Burmistrov I, et al. Conductivity of a carbon nanotubes-epoxy resin nanocomposite. IOP Conf Ser Mater Sci Eng Nov. 2019;693(1):012013. https://doi.org/10.1088/1757-899X/ 693/1/012013.
- [36] Roy S, Petrova RS, Mitra S. Effect of carbon nanotube (CNT) functionalization in epoxy-CNT composites. Nanotechnol Rev Dec. 2018;7(6):475–85. https://doi.org/ 10.1515/ntrev-2018-0068.
- [37] Wei J, Atif R, Vo T, Inam F. Graphene Nanoplatelets in Epoxy System: Dispersion, Reaggregation, and Mechanical Properties of Nanocomposites. J Nanomater 2015; 2015. https://doi.org/10.1155/2015/561742.
- [38] Atif R, Shyha I, Inam F. Mechanical, Thermal, and Electrical Properties of Graphene-Epoxy Nanocomposites—A Review. Polymers (Basel) Aug. 2016;8(8): 281. https://doi.org/10.3390/polym8080281.
- [39] Woldemariam MH, Belingardi G, Koricho EG, Reda DT. Effects of nanomaterials and particles on mechanical properties and fracture toughness of composite materials: a short review. AIMS Mater Sci 2019;6(6):1191–212. https://doi.org/ 10.3934/matersci.2019.6.1191.
- [40] Zare Y. Evaluation of nanoparticle dispersion and its influence on the tensile modulus of polymer nanocomposites by a modeling method. Colloid Polym Sci Feb. 2017;295(2):363–9. https://doi.org/10.1007/s00396-017-4016-x.
- [41] TA Instruments, 'Characterization of the Degree of Cure of Thermosetting Resins by DSC'. Accessed: Sep. 01, 2023. [Online]. Available: https://www.tainstruments. com/pdf/literature/TA389.pdf.
- [42] Bittmann B, Haupert F, Schlarb AK. Ultrasonic dispersion of inorganic nanoparticles in epoxy resin. Ultrason Sonochem 2009;16(5):622–8. https://doi. org/10.1016/j.ultsonch.2009.01.006.
- [43] Nam K-W, Moon C-K. Evaluation of dispersion degree of nanoparticles in TiO 2 /epoxy resin nanocomposites. Journal of Ocean Engineering and Technology Aug. 2014;28(4):338-44. https://doi.org/10.5574/KSOE.2014.28.4.338.
- [44] Al Wakeel S, Němeček J, Li L, Xi Y, Hubler M. The effect of introducing nanoparticles on the fracture toughness of well cement paste. Int J Greenhouse Gas Control May 2019;84:147–53. https://doi.org/10.1016/j.ijggc.2019.03.009.
- [45] Sasaki Y, Nishizawa Y, Watanabe T, Kureha T, Uenishi K, Nakazono K, et al. Nanoparticle-Based Tough Polymers with Crack-Propagation Resistance. Langmuir Jul. 2023;39(26):9262–72. https://doi.org/10.1021/acs.langmuir.3c01226.
- [46] Jen Y-M, Huang Y-C. Improvement in Tensile Quasi-Static and Fatigue Properties of Carbon Fiber-Reinforced Epoxy Laminates with Matrices Modified by Carbon

- Nanotubes and Graphene Nanoplatelets Hybrid Nanofillers. Nanomaterials Dec. 2021;11(12):3459. https://doi.org/10.3390/nano11123459.
- [47] Azimi HR, Pearson RA, Hertzberg RW. Fatigue of rubber-modified epoxies: effect of particle size and volume fraction. J Mater Sci Jul. 1996;31(14):3777–89. https://doi.org/10.1007/BF00352793.
- [48] Imanaka M, Motohashi S, Nishi K, Nakamura Y, Kimoto M. Crack-growth behavior of epoxy adhesives modified with liquid rubber and cross-linked rubber particles under mode I loading. Int J Adhes Adhes Jan. 2009;29(1):45–55. https://doi.org/ 10.1016/j.ijadhadh.2007.11.004.
- [49] Macosko CW. Fundamentals of Reaction Injection Molding. Oxford University Press; 1989.
- [50] Soulé ER, Borrajo J, Williams R.J. Thermodynamic Analysis of a Polymerization-Induced Phase Separation in Nanoparticle—Monomer—Polymer Blends. Macromolecules Oct. 2007;40(22):8082–6. https://doi.org/10.1021/ma071369c.
- [51] Huggins ML. Solutions of Long Chain Compounds. J Chem Phys May 1941;9(5): 440. https://doi.org/10.1063/1.1750930.
- [52] Flory PJ. Thermodynamics of High Polymer Solutions. J Chem Phys Jan. 1942;10 (1):51–61. https://doi.org/10.1063/1.1723621.
- [53] Zucchi IA, Galante MJ, Williams RJJ, Franchini E, Galy J, Gérard J-F. Monofunctional Epoxy-POSS Dispersed in Epoxy-Amine Networks: Effect of a Prereaction on the Morphology and Crystallinity of POSS Domains. Macromolecules Feb. 2007;40(4):1274–82. https://doi.org/10.1021/ma062188y.
- [54] Liu H, Zheng S, Nie K. Morphology and Thermomechanical Properties of Organic—Inorganic Hybrid Composites Involving Epoxy Resin and an Incompletely Condensed Polyhedral Oligomeric Silsesquioxane. Macromolecules Jun. 2005;38 (12):5088–97. https://doi.org/10.1021/ma0504318.
- [55] Demir MM, Castignolles P, Akbey Ü, Wegner G. In-Situ Bulk Polymerization of Dilute Particle/MMA Dispersions. Macromolecules Jun. 2007;40(12):4190–8. https://doi.org/10.1021/ma070142e.
- [56] Liu S, Li Y, Shen Y, Lu Y. Mechanical performance of carbon fiber/epoxy composites cured by self-resistance electric heating method. Int J Adv Manuf Technol Aug. 2019;103(9–12):3479–93. https://doi.org/10.1007/s00170-019-03707-0
- [57] Yang Z, Xie Y, He J, Wang F, Zeng X, Ma K, et al. A Comparative Study on the Mechanical Properties and Microstructure of Cement-Based Materials by Direct Electric Curing and Steam Curing. Materials Dec. 2021;14(23):7407. https://doi. org/10.3390/ma14237407.
- [58] S. Liu, Y. Li, S. Xiao, and T. Wu, 'Self-resistive electrical heating for rapid repairing of carbon fiber reinforced composite parts', 10.1177/0731684419832793, vol. 38, no. 11, pp. 495–505, Feb. 2019, 10.1177/0731684419832793.